Predator-Prey relationships in the Nutritional State-Structured Model of foraging behavior

Katja Della Libera

Christopher Kempes

Santa Fe Institute

Abstract

Trade-offs between reproduction, somatic expenses, growth, food storage, migration, and many more behaviors are fundamental to understanding organisms of all sizes and taxa. Understanding the evolution of the "choices" made between these trade-offs will allow us to gain further insights into the ecosystems of our world, to build predictive models, and even prescribe conservation policies

In 2018, Yeakel, Kempes, and Redner introduced a population dynamic model using a state-structured approach taking the form of first-order differential equations (Yeakel et al., 2018). The approach yielded promising results in predicting Cope's rule, Damuth's law, and an evolutionary mechanism for foraging behavior. Initial integration of competition showed the advantages and disadvantages of higher or lower body fat. Yet, a variety of behaviors, from food storage to predation, to the coexistence of herbivores competing for the same resource, to island ecology, or more complex food webs have not been considered to date.

Here we show an extension of the original nutritional state-structured model by increasing the trophic level to include a secondary predator.

We find that there are analytical solutions to the predicted steady-state of the new system of equations, however, the system does not reach this steady-state experimentally. Predator size and presence has almost no effect on the predicted steady-state for other trophic levels. The observed relationship between predator density and prey density is not predicted to be a power law with exponent 0.74 as predicted previously but has an exponent of 0.99 instead. This suggests the model does not capture the workings of a three trophic level interaction yet and more adjustments are needed.

In addition, we outline how accounting for differences in resource availability measured as net primary productivity and standing biomass can account for variation in data examined Yeakel et al. (2018).
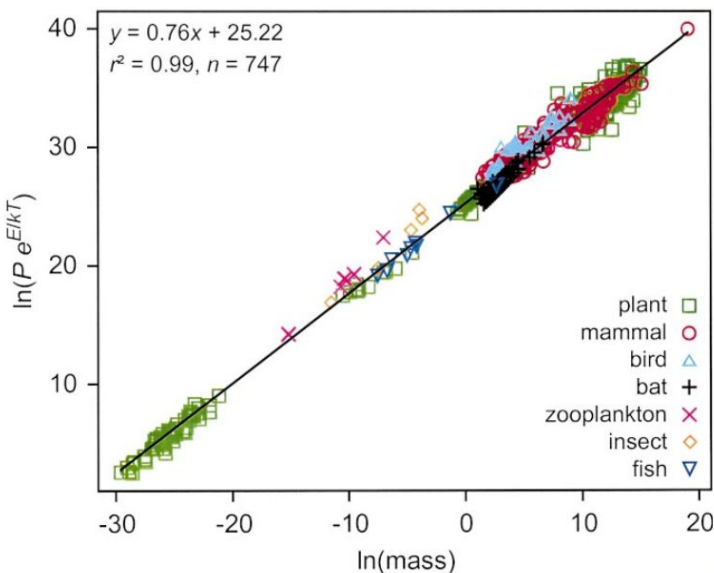
Introduction

Ecological modeling traditionally considered one level of exploration. Potentially the most famous of all, Lotka-Volterra, is an example of a differential equations model aiming to capture the broader-scale dynamics of population density over time (Lotka, 1926). The model consists of a set of differential equations modeling the change in a predator and prey population (Equation 1).

$$\frac{dx}{dt} = \alpha x - \beta xy$$ (1)

$$\frac{dy}{dt} = \delta xy - \gamma y$$

Equation 1: The original Lotka-Volterra model of population dynamics, where x represents the prey population, y is the predator population, and α, β, γ, and δ are parameters depending on the interaction of the two species.

Determining the parameter values for an ODE like Lotka-Volterra is where a second level of ecological modeling comes in. On the species level, more recent work has shown that many important factors such as metabolic rate, heart rate and more have a power-law relationship with the body mass of an individual of a specific species (Brown et al., 2004). Figure 1 shows an example of one of these relationships.

Figure 1: The temperature-corrected maximal whole-organism biomass production is related to the mass in grams of the organism through a power-law with exponent 0.76 (Brown et al., 2004)

Yeakel et al. (2018) took advantage of these relationships to use mass as the primary input to a novel type of ecological model that would allow us to predict population density based on mass and ecological conditions. What makes this approach even more compelling is the fact that density itself follows a power-law relationship with mass, as stated in Damuth's law (Damuth, 1987), who collected data from several hundred independent studies across the world as seen in figure 2.

ALLOMETRY OF POPULATION DENSITY
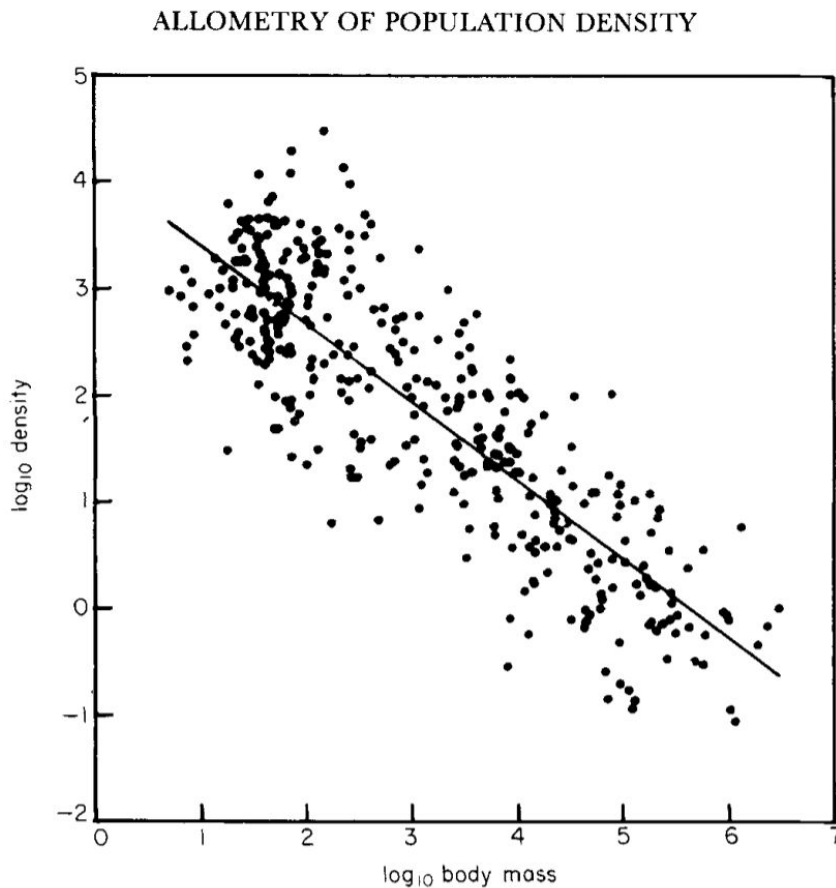
Figure 2: The density fo the smallest mammalian primary consumers at just 10s of grams is significantly higher than those of large consumers with millions of grams. The relationship is a power law (Damuth, 1987).

As seen in figure 3, the model proposed by Yeakel et al. (2018) offered an excellent fit to Damuth's law. While this is a promising result, the model can be expanded to include several extensions, perhaps most importantly the addition of further trophic levels to allow for

predator-prey relationships not included in the original model but known to have a significant impact in natural ecosystems. In addition, I will argue for the inclusion of two inputs in addition to mass to explain some of the variations in Damuth's data and suggest how to test the resulting hypothesis.
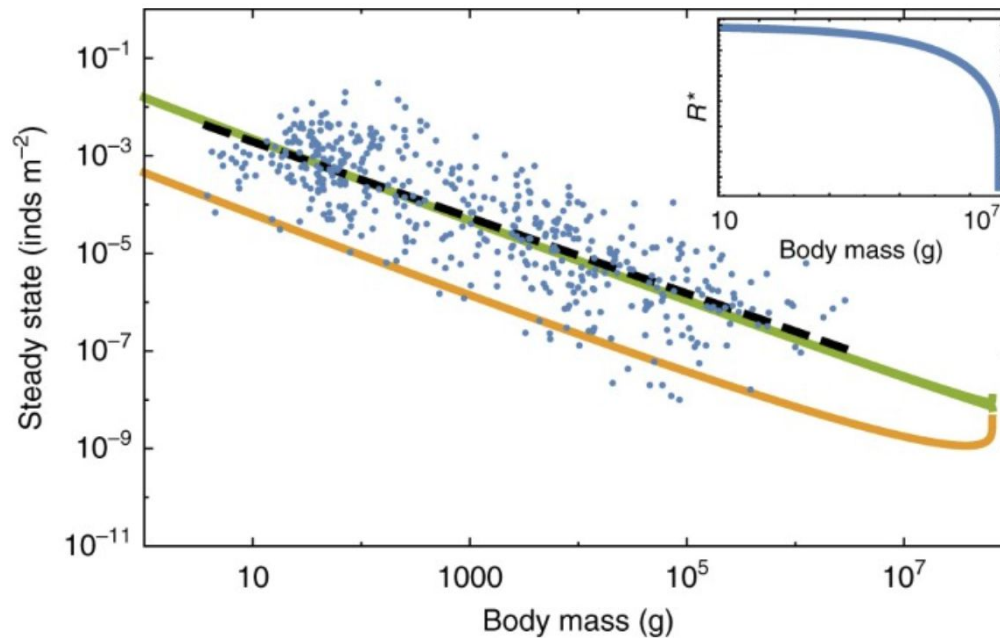

Figure 3: A plot showing the original model in Yeakel et al. closely matches the power-law relationship observed by Damuth (Yeakel et al., 2018).

Methods

The original model from Yeakel et al. (2018) can be seen in equation 2 and some of the parameters explained in Table 1. In summary, there are two nutritional states of the mammalian herbivore, full and hungry, of which only the full one is able to reproduce and only the hungry one will die (of starvation). The resource density determines how many of the consumers move from the hungry to the full state and vice versa.

$$\dot{F}_d = \lambda_{\max} F_d + \rho_{\max} R_d H_d / k - \sigma \left(1 - \frac{R_d}{C}\right) F_d,$$

$$\dot{H}_d = \sigma \left(1 - \frac{R_d}{C}\right) F_d - \rho_{\max} R_d H_d / k - \mu H_d,$$

$$\dot{R}_d = \alpha R_d \left(1 - \frac{R_d}{C}\right) -$$

$$\left[\left(\frac{\rho_{\max} R_d}{Y_H k} + P_H\right) H_d + \left(\frac{\lambda_{\max}}{Y_F} + P_F\right) F_d\right].$$

(2)

Equation 2: The original ODE from Yeakel et al (2018). An overview of the parameters is given in table 1.

Variable	Meaning	Variable	Meaning
F_d	Full consumer density	σ	Starvation rate
H_d	Hungry consumer density	C	Carrying capacity
R_d	Resource density	μ	Starvation death rate
λ_{max}	Reproduction rate	α	Intrinsic resource growth rate
ρ_{max}	Recovery rate	Y_x	Yield coefficient (grams of consumer produced per gram of resource)
k	Half-saturation constant	P_x	Maintenance rate of resource consumption

Table 1: Overview of the variables and parameters used in the original model, as well as their units

$$\dot{F}_{C_d} = \lambda_{C_{\max}} F_{C_d} + \frac{\rho_{C_{\max}}(F_d + H_d) H_{C_d}}{k_C} - \sigma_C \left(1 - \frac{(F_d + H_d)}{\theta(F^* + H^*)}\right) F_{C_d}$$

$$\dot{H}_{C_d} = \sigma_C \left(1 - \frac{(F_d + H_d)}{\theta(F^* + H^*)}\right) F_{C_d} - \frac{\rho_{C_{\max}}(F_d + H_d) H_{C_d}}{k_C} - \mu_C H_{C_d}$$

(3.1)

$$\dot{F}_d = \lambda_{\max} F_d + \frac{\rho_{\max} R_d H_d}{k} - \sigma \left(1 - \frac{R_d}{C}\right) F_d - \left[\left(\frac{\rho_{C_{\max}}(F_d + H_d)}{Y_H k} + P_{H_C}\right) H_{C_d} + \left(\frac{\lambda_{C_{\max}}}{Y_{F_C}} + P_{F_C}\right) F_{C_d}\right] \frac{F_d}{(F_d + H_d)}$$

(3.2)

$$\dot{H}_d = \sigma_H \left(1 - \frac{R_d}{C}\right) F_d - \frac{\rho_{\max} R_d H_d}{k_H} - \mu H_d - \left[\left(\frac{\rho_{C_{\max}}(F_d + H_d)}{Y_{H_C} k_c} + P_{H_C}\right) H_{C_d} + \left(\frac{\lambda_{C_{\max}}}{Y_{F_C}} + P_{F_C}\right) F_{C_d}\right] \frac{H_d}{(F_d + H_d)}$$

$$\dot{R_d} = \alpha\, R_d\left(1 - \frac{R_d}{C}\right) - \left[\left(\frac{\rho_{H_{max}}}{Y_H\, k_H}\frac{R_d}{} + P_H\right)H_d + \left(\frac{\lambda_{H_{max}}}{Y_F} + P_F\right)F_d\right] \qquad (3.3)$$

Equation 3: The extension of the model presented in Equation 2. Many of the parameters in the new carnivore trophic level(3.1) are analogous to the ones in the original model. The primary consumer level is extended to include death through predation.
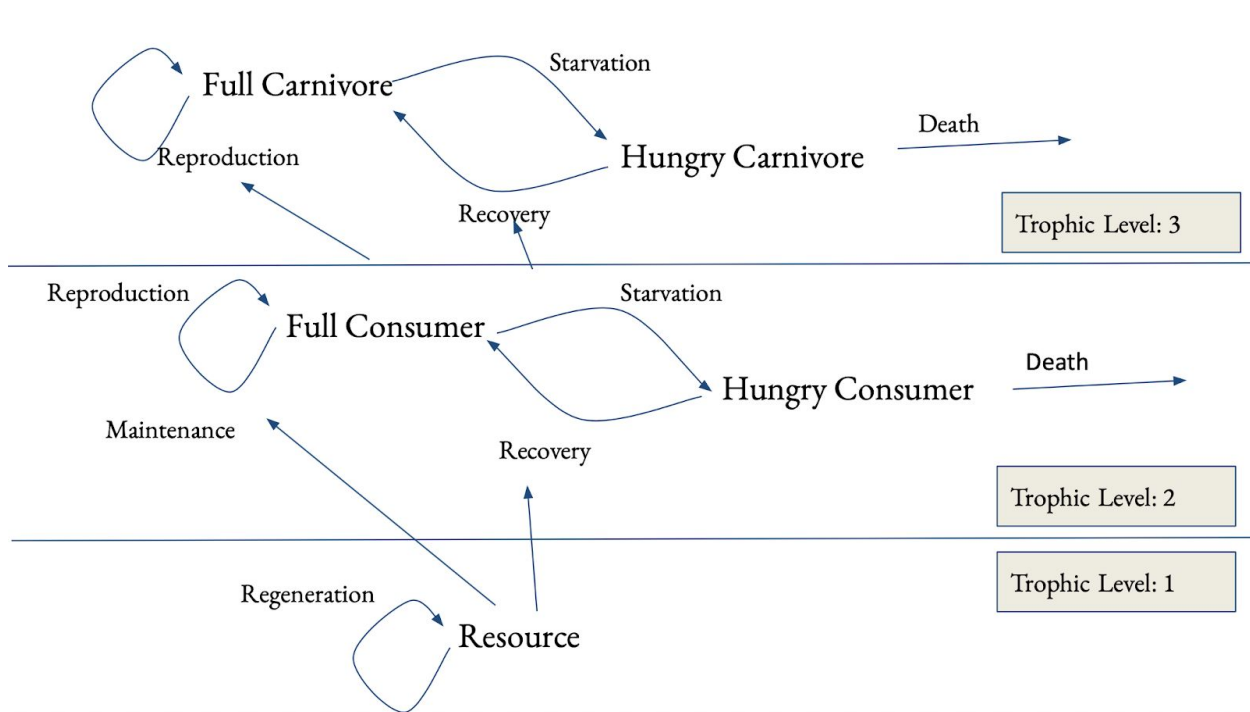

Figure 4: A graphic explaining the processes present in the system.

Equation 3 shows the extended ODE including a third trophic level and is illustrated graphically in figure 4. Consumption of herbivores is presumed to be proportional to the population of full and hungry herbivores respectively. F^* and H^* represent the original steady-state of the system and θ is a new parameter allowing one to rescale the carrying capacity.

Next, the system in equation 3 is non-dimensionalized and simplified using the rescaling $F = fF_d$, $H = fH_d$, $R = qR_d$, $F_c = f\,F_{c_d}$, $H_c = fH_{c_d}$ and $t = st_d$.

$$\dot{F_C} = \frac{1}{s}\left(\lambda_{C_{max}} F_C + \frac{\rho_{C_{max}} (F+H) H_C}{f\, k_C} - \sigma_C\left(1 - \frac{(F+H)}{\theta(F^*+H^*)f}\right) F_C\right)$$

$$\dot{H_C} = \frac{1}{s}\left(\sigma_C\left(1 - \frac{(F+H)}{\theta(F^*+H^*)f}\right) F_C - \frac{\rho_{C_{max}} (F+H) H_C}{f\, k_C} - \mu_C H_C\right)$$

$$\dot{F_H} = \frac{1}{s}\left(\lambda_{max} F + \frac{\rho_{H_{max}} R H}{k\, q} - \sigma_H\left(1 - \frac{R}{C_R q}\right) F_H - \left[\frac{\left(\frac{\rho_{C_{max}}(F+H)}{Y_{HC}\, k_C\, f} + P_{H_C}\right) H_C + \left(\frac{\lambda_{C_{max}}}{Y_{FC}} + P_{F_C}\right) F_C}{f}\right]\frac{F f}{(F+H)}\right)$$ (4)

$$\dot{H_H} = \frac{1}{s}\left(\sigma\left(1 - \frac{R}{C_R q}\right) F - \frac{\rho_{max} R H}{k\, q} - \mu H - \left[\frac{\left(\frac{\rho_{max}(F+H)}{Y_{HC}\, k_C\, f} + P_{H_C}\right) H_C + \left(\frac{\lambda_{C_{max}}}{Y_{FC}} + P_{F_C}\right) F_C}{f}\right]\frac{H f}{(F+H)}\right)$$

$$\dot{R} = \frac{1}{s}\left(\alpha R\left(1 - \frac{R}{C_R q}\right) - \frac{q}{f}\left[\left(\frac{\rho_{max} R}{Y_H\, k\, q} + P_H\right) H + \left(\frac{\lambda_{max}}{Y_F} + P_F\right) F\right]\right)$$

Equation 4: The formally non-dimensionalized version of equation (3)

If we then choose $s = 1$, $q = 1/C$, $f = 1/Y_H k$, drop the "max" subscripts for simplicity, and let $\xi = C/k$, $\delta = Y_H k P_H / C$, $\beta = Y_H k(\frac{\lambda}{Y_F} + P_F)/C$, $c_1 = \frac{\rho_c}{k_c}$, $c_2 = \frac{Y_H k}{\theta(F^*+H^*)}$, $c_3 = \frac{Y_H k}{Y_{Hc} k_c}$, and $c_4 = \frac{\lambda_c}{Y_{Fc}} + P_{F_C}$. We get the final simplified system seen in equation 5.

$$\dot{F_C} = \lambda_C F_C + c_1(F+H) H_C - \sigma_C(1 - c_2(F_d + H_d)) F_{C_d}$$

$$\dot{H_C} = \sigma_C(1 - c_2(F_d + H_d)) F_{C_d} - c_1(F+H) H_C - \mu_C H_{C_d}$$

$$\dot{F} = \lambda F + \rho \xi R H - \sigma(1-R) F - \left[(c_3(F+H) + P_{H_c}) H_C + c_4 F_C\right]\frac{F}{(F+H)}$$ (5)

$$\dot{H} = \sigma(1-R) F - \rho \xi R H - \mu H - \left[(c_3(F+H) + P_{H_c}) H_{C_d} + c_4 F_C\right]\frac{H}{(F+H)}$$

$$\dot{R} = \alpha R(1-R) - \left[(\rho R + \delta) H + \beta F\right]$$

Equation 5: The final, simplified system of equations.

Results

Analytically, one can solve for the expected steady-state for the carnivores, herbivores and the resource. Figure 5 shows the expected population densities of full carnivores and full herbivores depending on mass. The predator biomass has little impact on the expected values of either population.
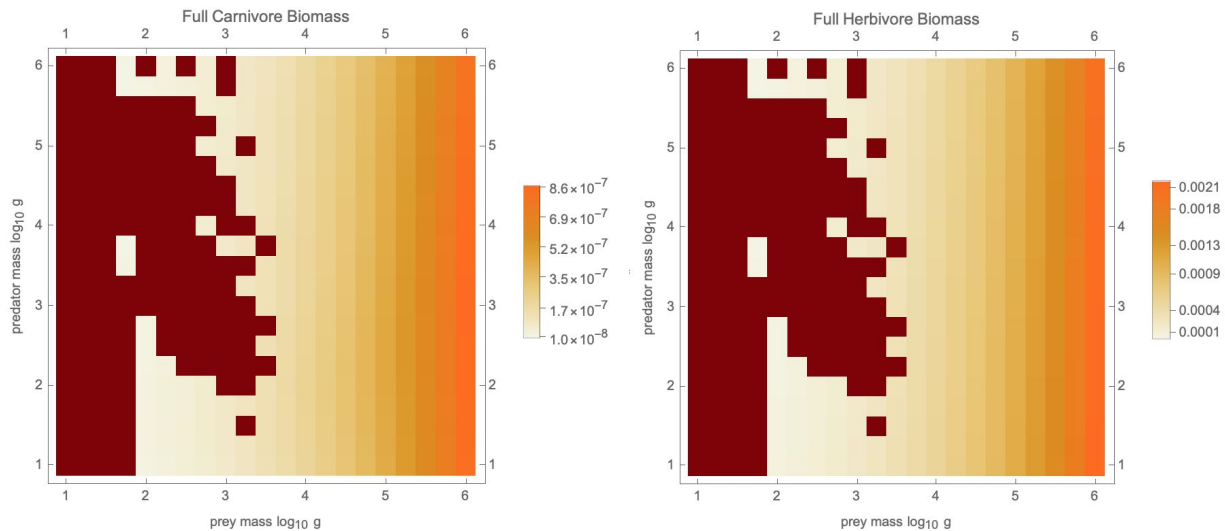
Figure 5: Two plot showing the carnivore density (left) and herbivore density (right) in relative density units depending on both predator and prey mass. At low prey mass, no steady-state is found, and predator mass does not have a large impact on the steady-state of the system.

Another interesting question to answer with the predicted steady-state data is what the relationship between expected predator density and prey density is. Hatton et al. (2015) collected a dataset on this relationship which shows a power-law relationship, as seen in figure 6. Figure 7 shows the data from figure 5 relating the predator and prey density in the same fashion as figure 6. The exponent is not close to 0.73 at 0.99, suggesting the model at its current state does not capture the effect observed in Hatton et al. (2015)
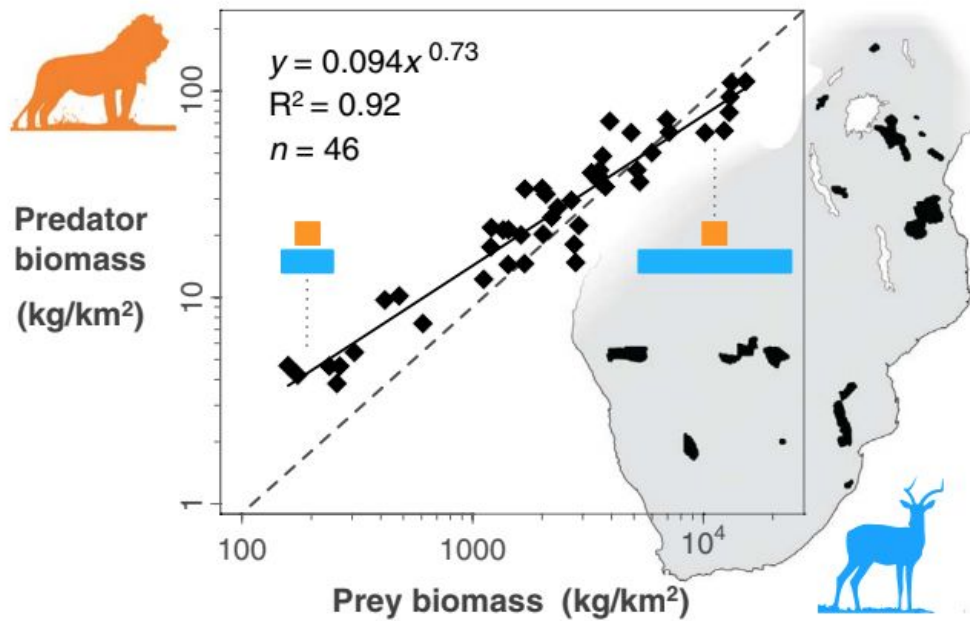
Figure 6: Predator density and prey density vary following a power law with an exponent of 0.73, meaning ecosystems become more bottom-heavy (Hatton et al., 2015)
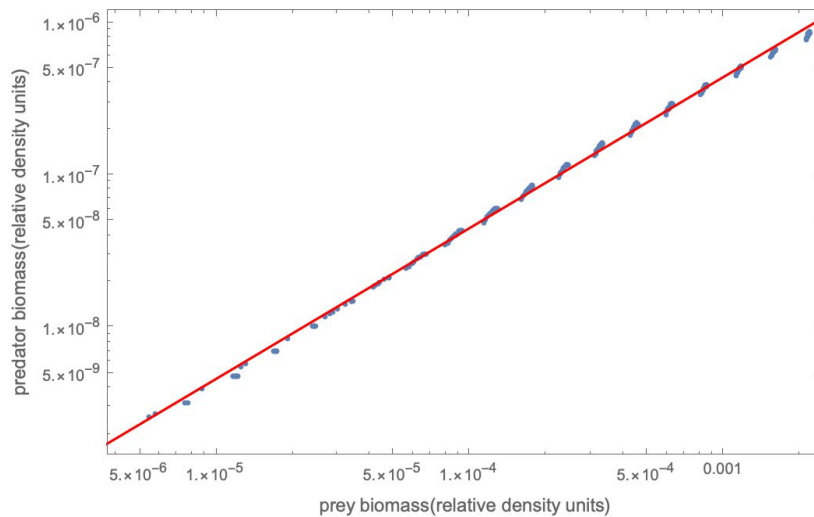

Figure 7: Relating the total biomass of predator and prey predicted for the model at different masses for each, shows a relationship with an exponent close to 1 (0.99). The model does not capture the 0.73 observed exponent by Hatton et al.,(2015)

Along with the expected result obtained through analytically solving the ODE, we started the system close to this expected steady-state to see its actual behavior. Unlike the original

NSM (Yeakel et al., 2018), the system does not stabilize at the steady-state, likely due in part to numerical errors. An example of this behavior can be seen in figure 8.
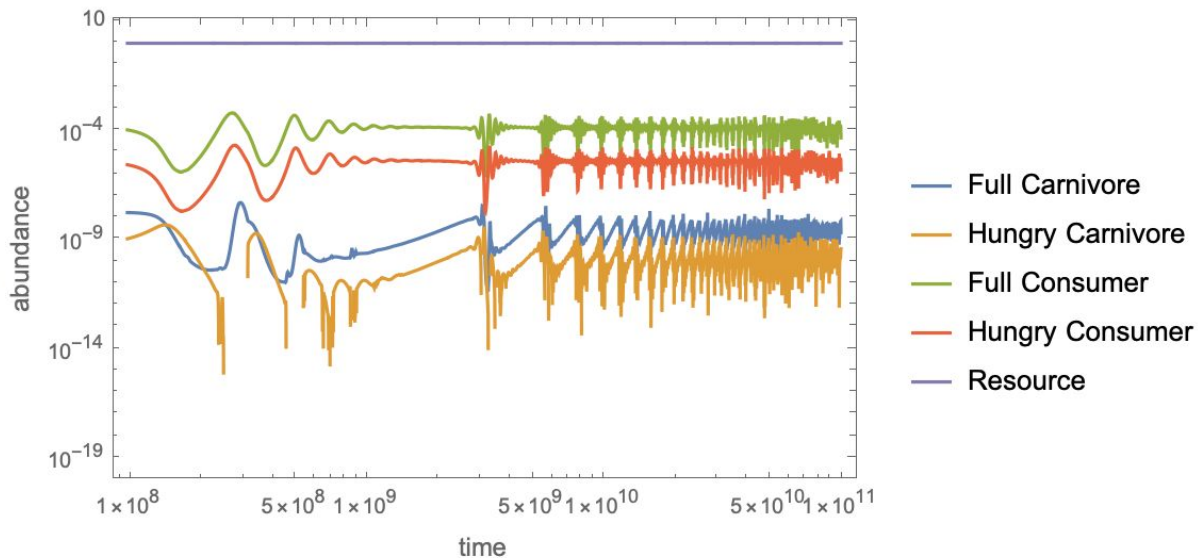
Figure 8: Even when starting at or close to the predicted steady-state, the system does not reach it and is unstable, showing oscillations in all populations other than the resource.

NPP and Carrying Capacity

Returning to the findings shown in figure 3, the original NSM can likely be improved by taking into account two factors independent of organism mass. The first is carrying capacity which can be approximated as standing biomass in an ecosystem and varies widely from dessert ecosystems to tropical rainforests. The second is net primary productivity, which directly influences α in the model by measuring the growth rate of an ecosystem. This value can vary seasonally as well as geographically across ecosystems. A change of about three orders of magnitude is sufficient to explain the majority of variability in the Damuth dataset, which is consistent with the observed range on earth
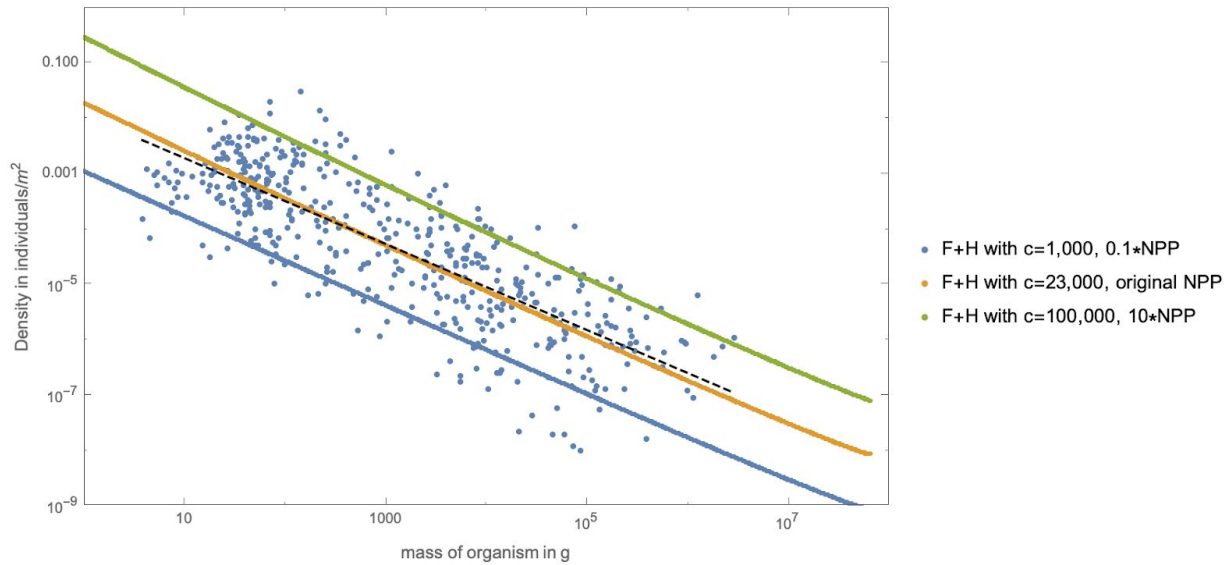
Figure 9: The original model in the center in orange and two variations thereof showing the upper and lower bounds of net primary productivity and carrying capacity. Three orders of magnitude are sufficient to explain a large amount of variation in the Damuth dataset.

Discussion

As Yaekel et al. (2018) suggest, there is great potential in using mass as a central component in determining the parameters used for a population density model of ecology. However, to include additional trophic levels, the parameters outlined in the original paper will likely have to be adjusted further to be able to reach the steady-state. Most likely candidates are yield coefficients as well as growth, which requires a more in-depth exploration of the literature on carnivores rather than primary consumers. Additional complexity may also help stabilize the system enough to do so. To capture the relationship between predator and prey density explored in Hatton et al., more adjustments are also likely needed.

References

Brown, J. H., Gillooly, J. F., Allen, A. P., Savage, V. M., & West, G. B. (2004). Toward a

    Metabolic Theory of Ecology. *Ecology, 85*(7), 1771–1789.

Damuth, J. (1987). Interspecific allometry of population density in mammals and other animals:

    The independence of body mass and population energy-use. *Biological Journal of the*

    Linnean Society, 31(3), 193–246. https://doi.org/10.1111/j.1095-8312.1987.tb01990.x

Hatton, I. A., McCann, K. S., Fryxell, J. M., Davies, T. J., Smerlak, M., Sinclair, A. R. E., &

    Loreau, M. (2015). The predator-prey power law: Biomass scaling across terrestrial and

    aquatic biomes. *Science Magazine, 349*(6252). https://doi.org/10.1126/science.aac6284

Lotka, A. J. (1926). Elements of Physical Biology. *Science Progress in the Twentieth Century*

    (1919-1933), 21(82), 341–343.

Yeakel, J. D., Kempes, C. P., & Redner, S. (2018). Dynamics of starvation and recovery predict

    extinction risk and both Damuth's law and Cope's rule. *Nature Communications, 9*(1),

    657. https://doi.org/10.1038/s41467-018-02822-y